

# The Bending Behaviour of Prestressed Masonry Box Beams at Ultimate

E.O.L. WILLIAMS, B.Eng.

M.E. PHIPPS, BSc.Tech., PhD, C.Eng., MICE, M.I.Struct.E.

University of Manchester Institute of Science and  
Technology, Manchester, England.

## SYNOPSIS

Six full sized post-tensioned prestressed masonry box beams 4.8m long have been tested under four point loading in a laboratory at the University of Manchester Institute of Science and Technology, England. This paper describes the results of these tests, proposes a method for predicting the ultimate bending behaviour of post-tensioned prestressed masonry box beams and gives design guidance. The implications this work has on the ultimate strength of post-tensioned diaphragm walls is emphasised.

## NOTATION

### Dimensions

- $A_s$  Area of tendon.  
 $b$  Width of beam flange.  
 $b_w$  Width of two webs of beam.  
 $d$  Effective depth of beam from top of beam to centre of tendon.  
 $d^1$  Effective depth of beam without cross ribs after bending.  
 $h_f$  Thickness of beam flange.  
 $l$  Beam span.  
 $x$  Depth to neutral axis.

### Moments and Forces

- $M$  Moment applied to beam.  
 $M_{cr}$  Moment at first cracking of masonry.  
 $M_u$  Ultimate moment.  
 $P$  Prestress Force.

### Stresses

- $f_e$  Effective prestress.  
 $f_k$  Characteristic compressive strength of masonry.  
 $f_s$  Stress in tendon at ultimate.  
 $f_{sb}$  Stress in tendon due to bending.  
 $f_{sl}$  Loss in tendon stress due to beam deflection in beams without cross ribs.

### Strains

- $\epsilon_b$  Average extreme fibre compression strain in masonry.  
 $\epsilon_{bt}$  Effective or average tensile masonry strain at depth  $d$  due to bending.

- $\epsilon_{bu}$  Ultimate compressive masonry strain due to bending.
- $\epsilon_{sb}$  Strain in tendon due to bending.
- $\epsilon_{sl}$  Loss in tendon strain due to beam deflection in beams without cross ribs.
- $\epsilon_t$  Average extreme fibre tension strain in masonry.

### Deflections and Rotations

- $a$  Beam deflection.
- $a_u$  Ultimate beam deflection.
- $\delta$  Tendon movement in beams.
- $\delta_u$  Ultimate tendon movement in beams without cross ribs.
- $\theta$  Overall beam rotation.

### Dimensionless Factors and Constants

- $E_s$  Young's Modulus for steel tendon.
- $K_1$  Deflection coefficient.
- $K_2$  Rotation coefficient.
- $M_1$  Moment coefficient =  $\frac{M_u}{f_k b d^2}$
- $M_{1E}$  Experimental value of  $M_1$
- $s$  Section coefficient =  $\frac{b-b_w}{(\frac{b-b_w}{b_w})} \frac{h_f}{d}$
- $x_1$  Neutral axis depth factor.
- $\alpha$  Force coefficient related to flexural compressive strength of masonry.
- $\beta$  Bond factor.
- $\gamma$  Effective depth coefficient.
- $\rho$  Effective prestress coefficient.

### INTRODUCTION

In designing prestressed masonry diaphragm walls a knowledge of the ultimate, or collapse limit state as well as the serviceability, or cracking limit is required. Full sized walls of this type can easily be tested under side loads up to the first tensile cracking(1) but testing to collapse, because of falling masonry, can be dangerous especially if the wall is large. It is, however, simple and safe to test horizontally spanning beams on the floor of the laboratory. Since a diaphragm wall can be considered to be a series of vertically spanning box beams its collapse load can be estimated from tests to failure of individual horizontally spanning masonry box beams.

When a masonry box beam (or diaphragm wall) is prestressed under the post-tensioning system the simplest place to put the tendons is inside the box cavity. If the cavity is continuous along the length of the beam then the deflection of the masonry and tendons will be

independent of one another (because of its size the cavity will not normally be grouted up). This is unlikely to be a problem under service loads but at ultimate the potential strength of the member can be impaired. The independent movements of the masonry and tendons can be prevented to some degree by the introduction of cross ribs, or webs, into the box section. These cross ribs do not materially hinder the ease of placement of the tendons and the performance of the beam is improved.

So far as is known the behaviour of prestressed masonry box beams has not been studied before. Thomas(2) and Plowman(3) tested to failure prestressed brickwork beams in which the high tensile steel wire tendons were threaded through perforations in the bricks and Curtin and Phipps(1) have tested prestressed diaphragm walls up to the first tensile cracking load.

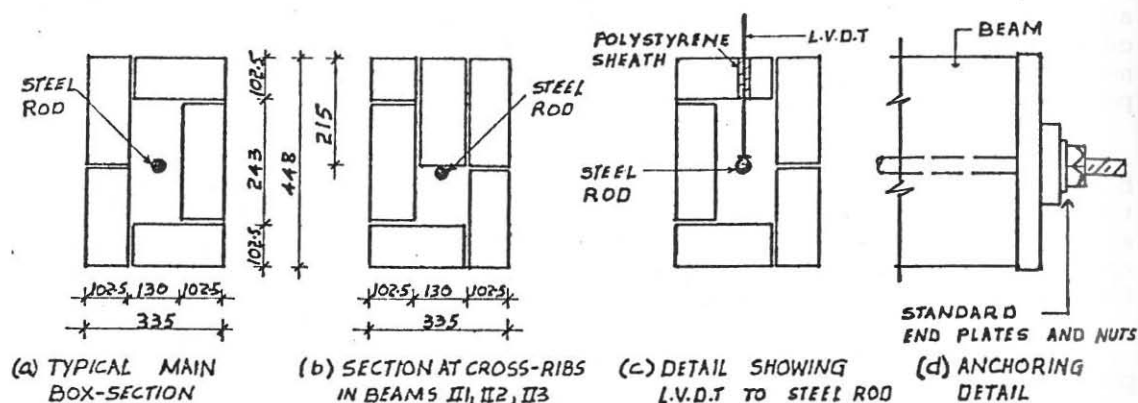
This paper describes tests on six full sized post-tensioned prestressed masonry box beams tested to their ultimate moment capacity. Three of the beams had cross ribs so as to maintain the position of the tendons right up to failure. The main purpose of the tests was to help to formulate design rules for the ultimate flexural limit state of prestressed diaphragm walls. A secondary consideration was to establish whether additional cross ribs can be advantageously used in such walls.

#### THE TESTS

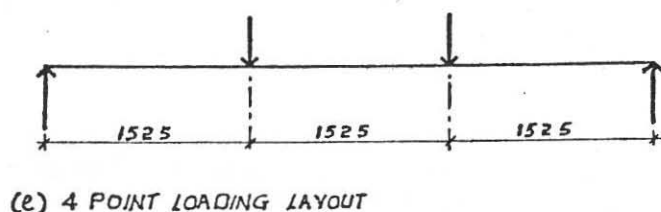
The six beams were tested under four point loading so that each beam had a region of constant bending moment. Beams I1, I2, I3 were constructed without cross ribs and beams II1, II2, II3 each had five cross ribs. The bricks were London Brick Company fletton Class III and the mortar was a nominal 1:1:6 cement, lime, sand mix. When the beams were at least 28 days old they were prestressed with one 40mm diameter Macalloy high tensile steel bar which was anchored at each end of the beams with a threaded nut bearing on a steel plate. To study the effects of the cross ribs the beams were grouped into pairs according to the level of prestress: I1 and II1 had high level prestress, I2 and II2 intermediate level prestress and I3 and II3 low level prestress. The depth of the beam section was chosen to be identical with the depth of the prestressed diaphragm walls of reference 1, i.e. 448mm, and the width of 335mm was chosen to fit the standard laboratory testing apparatus. The position of the prestressing tendon was chosen to match as nearly as possible that of the diaphragm wall tests(1). Figure 1 gives details of the beam construction.

Measurements of beam deformation and load were required at the ultimate moment capacity and beyond so an apparatus was used which, in conjunction with the laboratory strong floor, was stiff enough to prevent unstable failures. The use of non-return valves in the pressure lines of the jacks together with the high stiffness of the rig allowed the "frozen strain" technique to be used throughout the tests. The distance between the tension yokes was fixed at 1525mm because this was the distance between the strong points on the floor. The lengths of the two shear spans were chosen to be 1525mm to eliminate shear failures.

Strain measurements were taken in the constant moment region of the beams. LVDT transducers with gauge lengths of 65mm were used in continuous runs. LVDT's were also used to measure deflections



ALL DIMENSIONS IN MILLIMETRE



Details of beam construction

Fig. 1

and electro levels were used to measure rotations. Electrical resistance strain gauges were put on the prestressing tendons so that the prestressing force could be determined throughout the tests. The tendon position in the vertical direction was monitored at the mid span point of the beams by an LVDT passing through a small hole in the in the mortar joint. The applied loads at the third points were measured with Elliott load cells. All the readings were collected by a Peekel Data Logger which gave punched tape output for transfer to a computer.

The probable load deflection performance of the beams was assessed before each test so that straining could be applied in increments of load up to the onset of non-linearity and thereafter in increments of deflection. About three to five minutes was allowed before scanning the gauges at each loading stage. The average testing time was two and half hours per beam. All the cracks were blacked in as they appeared.

To get a preliminary idea of the strength of the compression zones of the beams as well as constructing and testing 215 x 215 x 4

course high standard prisms and carrying out standard brick and mortar tests five hollow box section prisms were tested. The cross section of the hollow prisms was identical to that of the beams but their heights varied from 290mm to 1500mm. They were tested in axial compression in a standard 2500kN Avery compression machine. Strains in the vertical and horizontal directions were measured using the same LVDT's as for the beam tests.

#### Behaviour of beams under test

In general the beams behaved like unbonded prestressed concrete beams with a few tension cracks forming at the tension face of the beam after the elimination of the initial compressive stress. With increased loading the cracks increased in number, got wider and propagated towards the compression face of the beam. Final failure was by crushing of the brickwork under compression. None of the beams failed in shear although one had a slight shear crack on one face. There was one exception to the general pattern and that was beam I1, the beam without cross ribs and with high prestress. It behaved as a slender compression member, buckling laterally under load and the first crack was a crack on the compression face of the beam.

The tension cracks occurred at the brick mortar interface. The cracks causing compression failure were roughly parallel to the axes of the beams, passed through the bricks and were opposite the tension cracks. In the beams without cross ribs the position of the compression failure was developed at an early stage after tensile cracking when very high compression strains were concentrated over a small length of the beam. The effect of the cross ribs was to distribute these high strains over a greater beam length and only near ultimate did the small failure zone length become dominant.

The cross ribs were effective in preventing the prestressing tendon moving towards the top flange. In all cases the prestress force did not appreciably increase with bending until after the tension cracks had formed (it should be noted here however that beam I2 was accidentally cracked in tension before testing began so the prestress force increased from zero load onwards).

On unloading all the beams, except I1 which buckled, returned almost to their original straight position and the tendon prestress force became close to the prebending value.

#### Behaviour of box prisms under test

All the prisms failed due to vertical splitting cracks which were randomly spaced around the section.

#### THEORY

A bending theory is proposed to describe the behaviour of the beams at ultimate. It is assumed that the ultimate moment is determined by crushing of the brickwork and not by steel fracture and that the distribution of stress is uniform over the compression zone of the member. It is further assumed that brickwork has no strength in tension. Thus from figure 2:

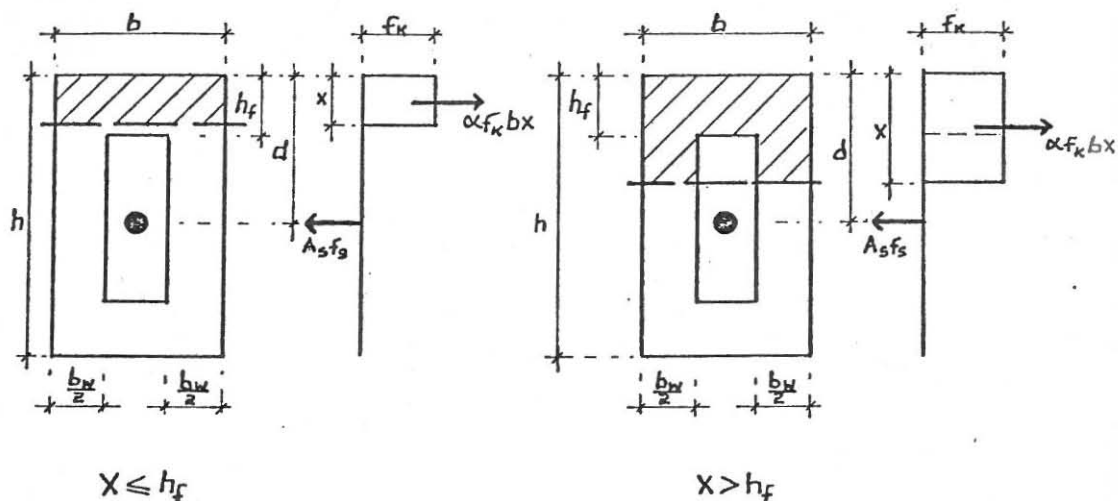


Fig. 2

resolving forces axially;

when  $x \leq h_f$

$$\alpha f_k b x = A_s f_s \quad \text{so} \quad x_1 = \frac{\rho}{\alpha} \cdot \frac{f_s}{f_e} \quad (1a)$$

$$\text{where } \rho = \frac{A_s f_e}{f_k b d}, \quad x_1 = \frac{x}{d}$$

similarly when  $x > h_f$

$$x_1 = \frac{\rho}{\alpha} \cdot \frac{f_s}{f_e} \cdot \frac{b}{b_w} - s \quad (1b)$$

$$\text{where } s = \left( \frac{b - b_w}{b_w} \right) \frac{h_f}{d}.$$

Taking moments about the centre line of the prestressing tendon,

when  $x \leq h_f$

$$M_u = \alpha f_k b x (d - 0.5x) \quad M_l = \alpha x_l (1 - 0.5 x_l) \quad (2a)$$

$$\text{where } M_l = \frac{M_u}{f_k b d^2}$$

similarly when  $x > h_f$

$$M_l = \alpha x_l (1 - 0.5 x_l) \frac{b_w}{b} + \alpha s (1 - 0.5 h_f) \frac{b_w}{d} \frac{b_w}{b} \quad (2b)$$

### Beams with cross ribs

For a given section and effective prestress with a fixed depth  $d$  equations (1) and (2) contain three unknowns  $\alpha$ ,  $x_l$  and  $f_s$  as well as the moment  $M_l$ .  $\alpha$  can be assumed to be  $0.75^4$  and strain compatibility will give a third equation.

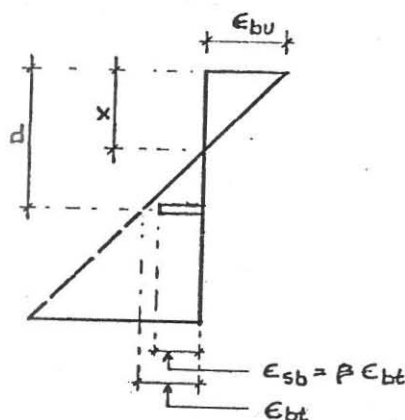


Fig. 3

Figure 3 shows the assumed linear distribution of strain across the brickwork section at failure due to bending only. The brickwork section is cracked and so linear strain distribution does not actually occur over the full depth of the beam at all cross sections. Over the whole length of the beam, however, on average plane sections do remain plane. Because the tendon is not bonded to the brickwork the tendon strain,  $\epsilon_{sb}$ , at a particular section is not the same as the strain in the brickwork at the same level,  $\epsilon_{bt}$ , but is some other value, i.e.

$$\epsilon_{sb} = \beta \epsilon_{bt}$$

where  $\beta$  is a bond factor.

For a beam with  $d$  constant over its length, that is for a beam with cross ribs, the average  $\epsilon_{bt}$  over the whole beam will equal  $\epsilon_{sb}$ . So the average value of  $\beta$  from one end of the beam to the other is unity. In the failure region where the moment is at the maximum value the brickwork strain will be higher than the average and so  $\beta$  at a section

undergoing failure is less than one. If it is assumed that the distribution of strain is the same as the bending moment diagram then,  $\beta$  can be taken to be 0.67 in the constant moment region of the beams under test.



From Figure 3

$$\frac{x}{d} = \frac{\epsilon_{bu}}{\epsilon_{bt} + \epsilon_{bu}} \quad \text{so} \quad x_1 = \frac{\beta \epsilon_{bu}}{\epsilon_{sb} + \beta \epsilon_{bu}}$$

$\epsilon_{sb}$  is the steel strain due to bending only and the stress associated with this strain is  $f_{sb}$  the steel stress due to bending. Therefore, providing  $f_{sb}$  is within the linear elastic range of the steel,

$$x_1 = \frac{E_s \beta \epsilon_{bu}}{f_{sb} + E_s \beta \epsilon_{bu}} \quad (3)$$

For low values of  $f_{sb}$   $x_1$  is sensitive to  $E_s \beta \epsilon_{bu}$  and this is difficult to quantify: an experimental result is needed.  $f_{sb}$  is related to  $f_s$  and  $f_e$  by

$$f_s = f_e + f_{sb} \quad \text{i.e.} \quad \frac{f_s}{f_e} = 1 + \frac{f_{sb}}{f_e} \quad (4)$$

#### Beams without cross ribs

For the beams without cross ribs the beam deflection causes differential movement between the masonry box and the prestressing tendon. If the tendon is assumed to remain straight then the relative displacement between the compression face of the beam and the tendon equals the beam deflection. Using the previous assumption that plane sections remain plane the deflection,  $a$ , can be assumed to be

$$a = K_1 \ell^2 \frac{\epsilon_{bu}}{x}$$

so the effective depth of the beam becomes,

$$d^1 = d - K_1 \ell^2 \frac{\epsilon_{bu}}{x}, \quad \text{or} \quad \frac{d^1}{d} = 1 - \gamma \frac{1}{x_1} \quad (5)$$

$$\text{where } \gamma = K_1 \epsilon_{bu} \left(\frac{\ell}{d}\right)^2.$$

$d^1$  has a minimum value of

$$d^1 = h_f + \frac{\phi_s}{2}$$

when the tendon is in contact with the underside of the compression flange.

Associated with the change in effective depth from  $d$  to  $d^1$  is a loss in the potential tendon strain at failure. If circular bending is assumed then the loss in tendon strain is



$$\epsilon_{sl} = 1 - \frac{\sin \theta}{\theta}$$

where on the previous assumptions,  $\theta = K_2 \ell \frac{\epsilon_{bu}}{x}$

and the associated loss in tendon stress is

$$f_{sl} = E_s \epsilon_{sl}$$

Equation (4) thus becomes:

$$\frac{f_s}{f_e} = 1 + \left( \frac{f_{sb}}{f_c} - \frac{f_{sl}}{f_e} \right) \quad (4a)$$

and the equations (2a) and (2b) become:

$$M_1 = \alpha x_1 \left( \frac{d^1}{d} - 0.5 x_1 \right) \quad (2c)$$

$$M_1 = \alpha x_1 \left( \frac{d^1}{d} - 0.5 x_1 \right) \frac{b_w}{b} + \alpha_s \left( \frac{d^1}{d} - 0.5 \frac{h_f}{d} \right) \frac{b_w}{b} \quad (2d)$$

respectively.

Both  $\gamma$  and  $\theta$  because of their dependence upon  $\epsilon_{bu}$  and  $x$  require to be assessed experimentally.

#### TEST RESULTS

The characteristic strength of the brickwork, calculated according to BS.5628 was 8.5 N/mm<sup>2</sup>. The average brick strength was 25.4 N/mm<sup>2</sup>, frog filled and 10.9 N/mm<sup>2</sup> frog unfilled. The 28 day mortar strength was 7.2 N/mm<sup>2</sup>.

Table 1 gives the results of the compression tests on the box prisms. It can be seen that, broadly speaking, the load carrying capacity is inversely proportional to the height of the specimens even though all the specimens are "short" from the buckling point of view. Also the results confirm that a characteristic strength of 8.5 N/mm<sup>2</sup> is a suitable value to use for the compression zones of the box beams.

Table 2 shows the values, at ultimate, of tendon stress,  $f_s$ , moment,  $M_u$ , central deflection,  $a_u$ , average surface compression strain in the constant moment region,  $\epsilon_{bu}$ , the change in the tendon position at the centre,  $\delta_u$  and the average neutral axis depth over the constant moment region,  $x_u$ . Also given is the effective pre-stress at the start of the test,  $f_e$  and the moment at which first tensile cracking was noticed,  $M_{cr}$ .

It can be seen from Table 2 that the ultimate moment capacity for the beams with cross ribs is more than twice the first cracking moment while for the beams without cross ribs the ultimate moment capacity is just less than twice the first cracking moment. Also

if the beams are paired according to the value of  $f_e$ , i.e. the three pairs I1 and III1, I2 and II2 and I3 and II3, the introduction of cross ribs raises the ultimate moment capacity of the beams by between 1.5 and 3.0 times.

TABLE 1 Compression Test Results on Box Section Prisms

Prisms	Height (m)	Cracking Load (kN)	Max. Load (kN)	Cracking Stress (N/mm <sup>2</sup> )	Max. Stress (N/mm <sup>2</sup> )	Ultimate Comp. Strain
4 courses	0.29	900	1480	7.6	12.49	0.0020
8 courses	0.60	900	1600	7.6	13.50	0.0031
14 courses	1.04	500	1195	4.22	10.09	0.0030
20 courses	1.50	500	900	4.22	7.6	0.0028

Figure 4 shows a plot of  $f_s/f_e$  against  $x$ , using experimental values. The sloping straight line drawn below the experimental points is an empirical representation of equations (3) and (4) (or (3) and (4a)). It is terminated at a maximum value of  $f_s/f_e = 1.5$  because this is thought to be a reasonable practical maximum value.

Table 3 tabulates experimental values of

$$\frac{M_u}{f_k b d^2} = M_{1E} \quad \text{and} \quad \frac{A_s f_e}{f_k b d} = \rho$$

for each beam and these values are plotted in Figure 5. Also in Figure 5 are plotted two curves which represent the theoretical predictions of  $M_1$  for values of  $\rho$  up to 0.6 for both types of beam. Theoretical values of  $M_1$  and  $\rho$  for the particular test beams are provided in Table 3 where it can be seen that there is good agreement between experiment and theory. The procedure for calculating the theoretical values is given below.

Equations (1a) and (1b) are superimposed on the empirical curve of Figure 4 for the particular value of  $f_e$  to give Figure 6. For any particular value of  $f_e$  the corresponding  $x_1$  is then given by the intercept of the curves. (It is immaterial whether the beam has cross ribs or not at this stage because  $d$  is not fundamentally part of equations (1a) and (1b)). With this value of  $x_1$   $M_1$  can be calculated from equations (2a) or (2b) for beams with cross ribs or (2c) or (2d) where cross ribs are absent. In equations (2c) and (2d)  $d^1/d$  has first to be calculated from equation (5) and to do this a value of  $\gamma$  is required. A suitable value was found to be

$$\gamma = 0.15.$$

The value of  $\alpha$  used throughout was 0.75.

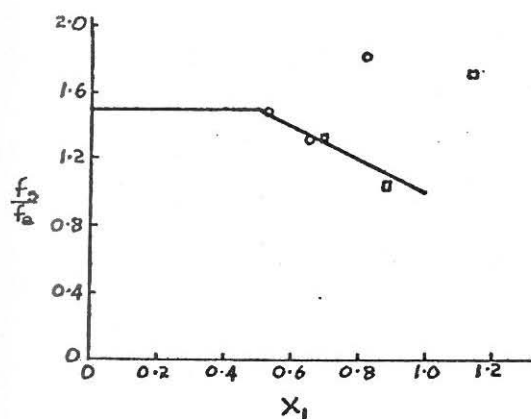
TABLE 2 Experimental values

Beam	$f_e$ N/mm <sup>2</sup>	$f_s$ N/mm <sup>2</sup>	$M_{cr}$ kN-m	$M_u$ kN-m	$a_u$ mm	$\epsilon_{bu}$ $\times 10^{-3}$	$x_u$ mm	$\delta_u$ mm	$\frac{M_u}{M_{cr}}$
I1	265	276	18.0	34.0	10.0	2.1	200	10	1.9
I2*	177	305	-	19.0	90.0	4.0	255	50	-
I3	118	156	12.0	22.8	13.3	1.5	155	17	1.9
II1	249	329	25.0	55.8	26.0	2.9	155	-	2.2
II2	178	262	22.4	57.0	19.3	1.6	123	-	2.6
II3	105	189	12.3	33.1	39.8	4.8	195	-	2.7

\* Beam I2 was cracked prior to testing so  $M_{cr}$  is unknown.

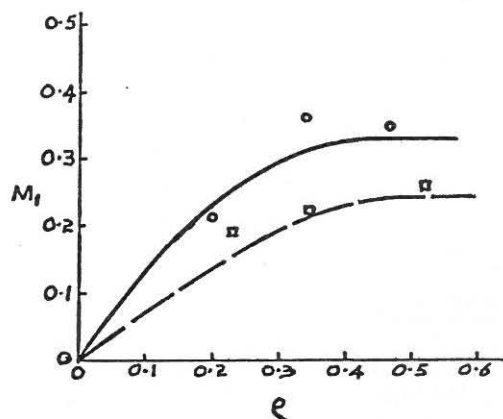
TABLE 3

Beam	$M_{1E}$	$\rho$	$M_1$	$\frac{M_{1E}}{M_1}$
I1	0.26	0.52	0.24	1.1
I2	0.22	0.35	0.21	1.0
I3	0.19	0.23	0.15	1.3
II1	0.35	0.47	0.33	1.1
II2	0.36	0.34	0.31	1.2
II3	0.21	0.20	0.23	0.9



○ TEST RESULT, BEAMS II1, II2, II3

□ TEST RESULT, BEAMS I1, I2, I3



○ TEST RESULT, BEAMS II1, II2, II3

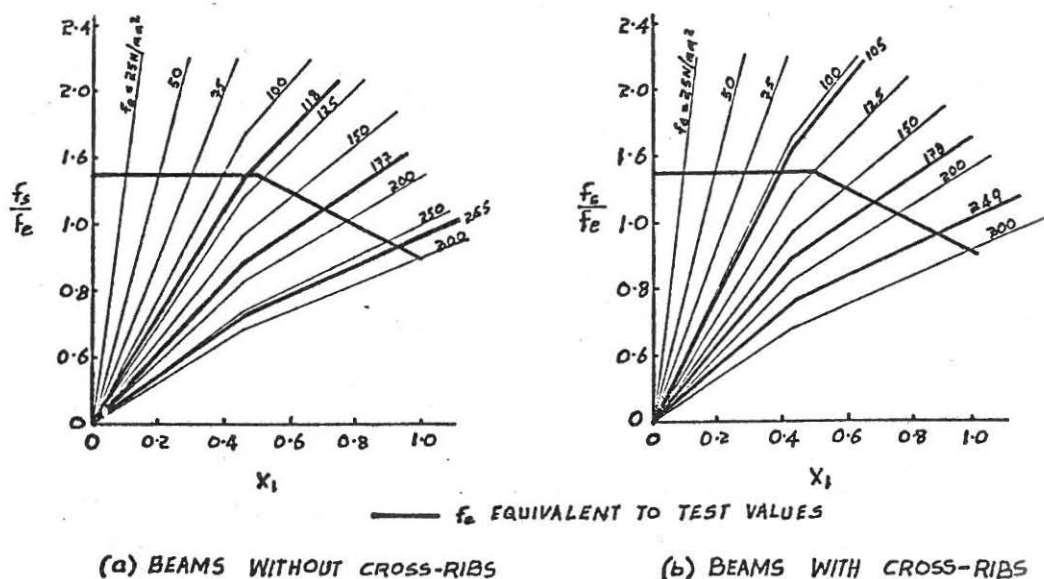
□ TEST RESULT, BEAMS I1, I2, I3

— THEORY CURVE FOR BEAMS WITH CROSS-RIBS

- - - THEORY CURVE FOR BEAMS WITHOUT CROSS-RIBS

Fig. 4

Fig. 5



## CONCLUSIONS

Fig. 6

1. The method proposed for calculating the ultimate moment capacity of prestressed masonry box beams gives accurate results within the range of the beams tested. It is simple to use and is suitable for a design office.
2. The effect of introducing cross ribs to maintain the position of the tendon is to increase the ultimate moment capacity of the box beams by at least 50%.
3. The ratio of ultimate moment to the moment at which first tensile brickwork cracks appeared had a minimum value of 1.9.
4. It is suggested that the results of this work are applicable to the ultimate bending strength of post-tensioned prestressed masonry diaphragm walls and that the ultimate strength of such walls can be improved by the introduction of cross ribs to maintain the position of prestressing tendons.

## REFERENCES

1. Curtin, W.G., Phipps, M.E., "Prestressed Masonry Diaphragm Walls", 6th I.B.Ma.C. Rome, 1982.
2. Thomas, K., "Post-stressed Brickwork Beams", Designing, Engineering and Constructing with Masonry Products, 1969, pp 285-288.
3. Plowman, J.M., "Post-stressed Brickwork Beams", Designing, Engineering and Constructing with Masonry Products, 1969, pp 288-295.
4. Beard, R., "A Theoretical Analysis of Loadbearing Brickwork in Bending", British Ceramic Society 7th Int. Symposium on Loadbearing Brickwork, London, Nov. 1980.